

In situ luminescence measurements of GaN/Al_2O_3 film under different energy proton irradiations

Wenli Jiang, Xiao Ouyang, Menglin Qiu, Minju Ying, Lin Chen, Pan Pang, Chunlei Zhang, Yaofeng Zhang, and Bin Liao

Citation: Chin. Phys. B, 2024, 33 (**5**): 058702. DOI: 10.1088/1674-1056/ad1b3f

What follows is a list of articles you may be interested in

Thermally enhanced photoluminescence and temperature sensing properties of $Sc_2W_3O_{12}:Eu^{3+}$ phosphors

Yu-De Niu(牛毓德), Yu-Zhen Wang(汪玉珍), Kai-Ming Zhu(朱凯明), Wang-Gui Ye(叶王贵), Zhe Feng(冯喆), Hui Liu(柳挥), Xin Yi(易鑫), Yi-Huan Wang(王怡欢), and Xuan-Yi Yuan(袁轩一)
Chin. Phys. B, 2023, 32 (**2**): 028703. DOI: 10.1088/1674-1056/ac70b8

Effects of 3.7 T–24.5 T high magnetic fields on tumor-bearing mice

Xiaofei Tian(田小飞), Ze Wang(王泽), Lei Zhang(张磊), Chuanying Xi(郗传英), Li Pi(皮雳), Ziping Qi(齐紫平), Qingyou Lu(陆轻铀), Xin Zhang(张欣)
Chin. Phys. B, 2018, 27 (**11**): 118703. DOI: 10.1088/1674-1056/27/11/118703

Spin-controlled directional launching of surface plasmons at the subwavelength scale

Tao Huang(黄韬), Jia-jian Wang(王佳见), Zi-wei Li(李梓维), Wei Liu(刘伟), Feng Lin(林峰), Zhe-yu Fang(方哲宇), Xing Zhu(朱星)
Chin. Phys. B, 2016, 25 (**8**): 087302. DOI: 10.1088/1674-1056/25/8/087302

Al-doping influence on crystal growth of Ni-Al alloy: Experimental testing of a theoretical model

Rong Xi-Ming (荣曦明), Chen Jun (陈骏), Li Jing-Tian (李菁田), Zhuang Jun (庄军), Ning Xi-Jing (宁西京)
Chin. Phys. B, 2015, 24 (**12**): 128706. DOI: 10.1088/1674-1056/24/12/128706

In situ luminescence measurements of GaN/Al_2O_3 film under different energy proton irradiations

Wenli Jiang(蒋文丽)[1], Xiao Ouyang(欧阳潇)[1], Menglin Qiu(仇猛淋)[1,2,†], Minju Ying(英敏菊)[1,2,‡], Lin Chen(陈琳)[1,2], Pan Pang(庞盼)[2], Chunlei Zhang(张春雷)[1,2], Yaofeng Zhang(张耀锋)[1,2], and Bin Liao(廖斌)[1,2]

[1] *Key Laboratory of Beam Technology of Ministry of Education, College of Nuclear Science and Technology, Beijing Normal University, Beijing* 100875, *China*
[2] *Institute of Radiation Technology, Beijing Academy of Science and Technology, Beijing* 100875, *China*

(Received 3 September 2023; revised manuscript received 2 January 2024; accepted manuscript online 5 January 2024)

Ion beam-induced luminescence (IBIL) experiments were performed to investigate the *in situ* luminescence of GaN/Al_2O_3 at varying ion energies, which allowed for the measurement of defects at different depths within the material. The energies of H^+ were set to 500 keV, 640 keV and 2 MeV, the Bragg peaks of which correspond to the GaN film, GaN/Al_2O_3 heterojunction and Al_2O_3 substrate, respectively. A photoluminescence measurement at 250 K was also performed for comparison, during which only near band edge (NBE) and yellow band luminescence in the GaN film were observed. The evolution of the luminescence of the NBE and yellow band in the GaN film was discussed, and both exhibited a decrease with the fluence of H^+. Additionally, the luminescence of F centers, induced by oxygen vacancies, and Cr^{3+}, resulting from the $^2E \rightarrow {}^4A_2$ radiative transition in Al_2O_3, were measured using 2 MeV H^+. The luminescence intensity of F centers increases gradually with the fluence of H^+. The luminescence evolution of Cr^{3+} is consistent with a yellow band center, attributed to its weak intensity, and it is situated within the emission band of the yellow band in the GaN film. Our results show that IBIL measurement can effectively detect the luminescence behavior of multilayer films by adjusting the ion energy. Luminescence measurement can be excited by various techniques, but IBIL can satisfy *in situ* luminescence measurement, and multilayer structural materials of tens of micrometers can be measured through IBIL by adjusting the energy of the inducing ions. The evolution of defects at different layers with ion fluence can be obtained.

Keywords: ion beam-induced luminescence (IBIL), GaN/Al_2O_3, ion beam

PACS: 87.15.mq, 78.55.Cr, 81.15.Jj **DOI:** 10.1088/1674-1056/ad1b3f

1. Introduction

Gallium nitride (GaN) is widely used due to its wide band gap at room temperature (3.4 eV). Due to the excellent properties of GaN, photoelectric devices based on GaN are in common use, for example, high electron mobility transistors and light-emitting diodes (LEDs).[1,2] The application of these devices is based on the understanding and modification of defects. GaN defects include intrinsic defects, unintentionally doped impurities formed during growth and impurity defects caused by doping. Intrinsic defects exist in the form of vacancies, interstitial atoms, substitutional atoms, color centers or antipositions. Complex defects are formed by the interaction of isolated intrinsic defects or the combination of intrinsic defects and impurities. These defects affect the electronic and optical performance of GaN devices and reduce the radiation efficiency and operating life of LEDs. The breakdown voltage of high-power electronic devices is also lower than the predicted value due to the effect of point defects. It is necessary to study these defects to maintain the stability of the devices.

In the context of GaN, investigations have been conducted on the near band edge (NBE) and yellow band luminescence in diverse GaN epilayers.[3,4] The NBE energy levels exhibited in different samples demonstrate a smaller difference, with this variation being attributed to factors such as the band gap and measurement temperature. It is pertinent to note that NBE emissions are linked to the recombination of excitons and the concentration of the donor and acceptor defects, and, in general, a lower presence of defects within the crystal corresponds to a stronger NBE peak and a higher degree of perfection the GaN crystal.[5] Furthermore, Reshchikov and colleagues have undertaken several comprehensive studies of the luminescence of the yellow band, which arises due to the recombination of several donor and acceptor defects and extended complex defects.[6–8] The process of luminescence measurement has been proved to be an effective method for studying crystal defects. Beyond assessing information about crystal quality, luminescence spectroscopy serves as a valuable tool for the identification and quantification of defects and impurities within semiconductor materials.

Al_2O_3 is renowned for its exceptional performance at elevated temperatures and serves as an outstanding electrical insulator, making it a preferred substrate for various semiconductor materials. Within the Al_2O_3 matrix, defects denoted as F centers, F^+ centers and F^{2+} centers are intrinsically linked to oxygen vacancies and have been the subject of extensive research, involving exposure to proton, electron,

[†]Corresponding author. E-mail: mlqiu@bnu.edu.cn
[‡]Corresponding author. E-mail: mjying@bnu.edu.cn

© 2024 Chinese Physical Society and IOP Publishing Ltd

neutron and heavy-ion irradiation.[9,12] The accumulation of oxygen vacancies, specifically the formation of F centers, is associated with the generation of aluminum colloids and concurrent surface electrical degradation.[13] Radiation exposure can engender the formation of Frenkel defects, primarily due to the nuclear stopping effect, while ionization processes can also induce structural damage within the crystal during radiation exposure.[14] Additionally, a series of ions, including chromium, nickel, ytterbium, erbium and yttrium, have been studied in the context of doping Al_2O_3. These studies aim to investigate and understand the optical properties and behavior resulting from the incorporation of these dopants.[12,15–17]

Multiple excitation methods are available for obtaining information on point defects. Deep-level transient spectroscopy, secondary-ion mass spectrometry analysis and positron annihilation spectroscopy are all used to study point defects in semiconductors. Compared with these measurement methods, photoluminescence (PL) meets the requirements of measuring shallow and deep-level defects and determining the concentration and the strength of electron–phonon coupling at the same time, but it involves irradiating samples with light, with a detection depth typically in the range of nanometers from the surface. Measurement of the effect of irradiation on semiconductors using PL is an *ex situ* measurement, and cannot obtain the evolution of point defects during irradiation. On the other hand, ion beam-induced luminescence (IBIL) can fulfill *in situ* measurement of semiconductors or nonconductors, and the type, structure and concentration of point defects can be obtained in real time. IBIL employs ion ionization and excitation, and by controlling the energy of the incident ions it allows precise control over the depth of incident ions to measure the luminescence at a specific depth. In addition to its use as an ion beam analysis technique, IBIL serves as an *in situ* measurement method for researching damage due to ion irradiation. This method leverages the interaction between ions and solid materials to excite transitions of the outer electrons, subsequently enabling analysis of the emission spectra generated by deexcitation. The detection limit of IBIL can reach parts per million (ppm) or even lower.[19] Moreover, the technology enables the analysis of changes in physical and chemical state in target atoms during irradiation.[20] The measurement principles of IBIL and PL differ, leading to variations in the observed luminescence spectra. In prior research at Beijing Normal University, various experiments have been successfully implemented in the IBIL measurement system to investigate the effects of flux and temperature on the luminescence of low-concentration rare earth elements and defects.[21–25] Branson *et al*. conducted a study on the luminescence of InGaN/GaN using IBIL, PL and cathodeluminescence measurement methods, and found that luminescence intensity depends on the specific excitation method employed in each measurement technique.[18]

In this study, IBIL spectra of GaN/Al_2O_3 at various depths were acquired by adjusting the incident ion energy to adapt to different film thicknesses. Subsequently, we conducted an in-depth analysis of the evolution of luminescence observed in GaN/Al_2O_3 during irradiation.

2. Experimental details and simulation

The GaN (0001) grown on Al_2O_3 (0001) utilized in the experiment was sourced from Suzhou Nanowin Science and Technology Company. GaN epitaxial deposition was performed by metal organic chemical vapor deposition. The thicknesses of the GaN epitaxial film and Al_2O_3 substrate were 4.5±0.5 μm and 430±25 μm, respectively. The normal temperature resistivity of GaN/Al_2O_3 at room temperature is below 0.05 Ω·cm and the carrier concentration is above 1×10^{18} cm^{-3}.

In irradiation experiments, Stopping and Range of Ions in Matter (SRIM) simulations play a pivotal role in assessing the interactions between ions and target materials. These simulations involve specifying the elemental composition and density of the target material and having knowledge of the ion type, direction of incidence, energy and charge. By inputting these parameters, SRIM simulations provide valuable insights into various aspects of ion interactions with the material, including energy transfer, depth of incidence, ion trajectory and ion distribution range. For materials with complex multilayer structures, such as GaN/Al_2O_3, SRIM simulations can be particularly valuable. By setting different incident ion energies, these simulations allow researchers to model the energy deposition positions of ions within distinct layers of the material. The simulation results can then be used to guide the parameter settings in actual experiments, providing insights into ion behavior at different depths and heterojunction interfaces. This approach enhances the understanding of ion–material interactions in intricate structures and aids in optimizing experimental designs for radiation studies.

In the SRIM simulation, GaN/Al_2O_3 is set with two layers. The GaN density is set to 6.1 g·cm^{-3} and the Al_2O_3 density is set to 4.0 g·cm^{-3}. The direction of incidence of H^+ is perpendicular to the GaN/Al_2O_3 surface, which is consistent with the IBIL experiments. The H^+ energy is set to 500 keV, 640 keV and 2 MeV, corresponding to the H^+ incidence depth of the GaN epilayer, GaN/Al_2O_3 heterojunction and Al_2O_3 substrate, respectively. S_e and S_n represent the deposited energy of ionization loss and the nuclear stopping energy loss, respectively. The energy loss distributions of 500 keV, 640 keV and 2 MeV H^+ are visualized in Fig. 1. It is observed that with increasing H^+ energy, the proportion of ionization loss energy (S_e) increases while the proportion of nuclear stopping loss energy (S_n) decreases. Specifically, for the three different

energies of H^+, S_e accounts for 99.72% (500 keV), 99.77% (640 keV) and 99.88% (2 MeV) of the total energy loss in GaN/Al_2O_3. This signifies that ionization loss becomes more dominant with higher incident H^+ energies. The simulation results also provide information on the range: H^+ with energies of 500 keV, 640 keV and 2 MeV reached depths of 3.96 μm, 5.34 μm and 27.6 μm, respectively. Notably, when using 2 MeV H^+ ions for measurement, approximately 12.42% of the total energy loss occurs in the GaN film. It is observed that S_e mainly plays the role of ionization and excitation. Nuclear stopping contributes to the creation of point defects by the loss of energy through collisions. The most significant lattice damage to the lattice occurs near the Bragg peak. The energy values of S_e vary within the range 12.1–18.5 eV·Å^{-1}, 9.6–17.8 eV·Å^{-1} and 5.25–5.8 eV·Å^{-1} within GaN film, corresponding to measurement with 500 keV, 640 keV and 2 MeV H^+ ions, respectively.

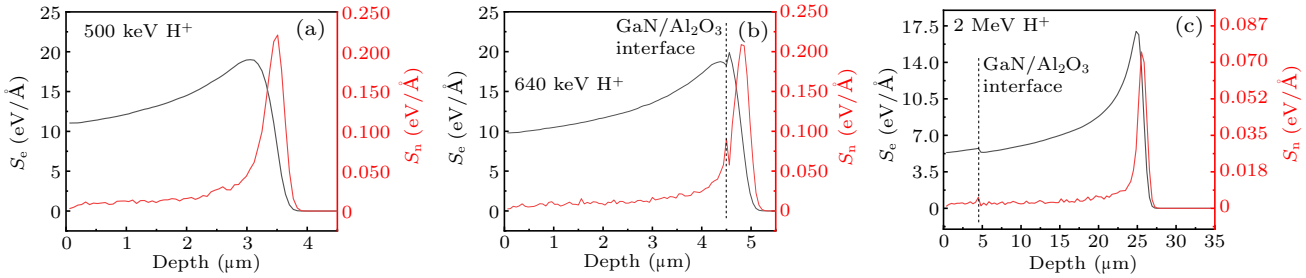


Fig. 1. Nuclear energy loss and electron energy loss with SRIM calculation of 500 keV, 640 keV and 2 MeV H^+ with GaN/Al_2O_3.

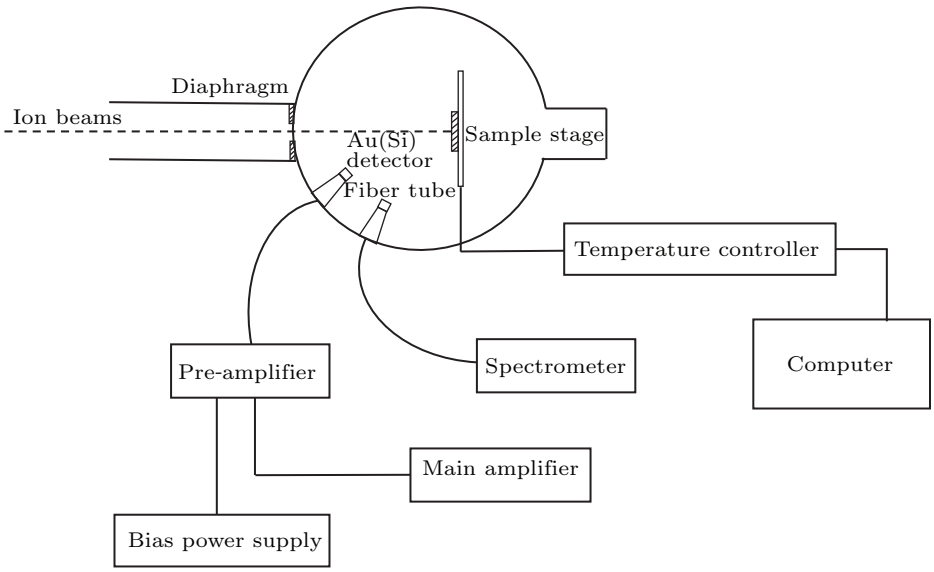


Fig. 2. Schematic diagram of the IBIL experimental setup.

The PL experiment was completed at the Suzhou Institute of Nano-Tech and Nano-Bionics. An He–Cd 325 nm laser was used in PL experiment, and the excitation power was set to 28 mW. Due to the limit of excitation power, the intensity of GaN with PL is too weak to distinguish at room temperature, thus the PL measurement was performed at 250 K. A schematic diagram of the IBIL experimental setup is shown in Fig. 2. The ion beam is accelerated by a GIC4117 2 × 1.7 MV tandem accelerator. After the ions have irradiated the sample, the emitted photons are transmitted through the optical fiber and received by the QE-Pro spectrometer. At the same time, spectral analysis software on the computer (OceanView) is used for spectral storage with an integration time of 0.5 s. To enhance the accuracy of the results, it is essential to monitor fluctuations in the beam current, as the production of backscattered ions is directly proportional to the beam intensity.[26] Therefore, the beam current is deliberately maintained below 20 nA to mitigate any potential heating effects. In the IBIL experiments, the energy of H^+ ions is specifically set at 500 keV, 640 keV and 2 MeV in accordance with the results obtained from SRIM simulations.

3. Results and discussion

As depicted in Fig. 3, the *in situ* luminescence of GaN/Al_2O_3 was investigated with 500 keV, 640 keV and 2 MeV H^+ from 200 nm to 1000 nm. Through SRIM simulation calculations, it was found that in GaN/Al_2O_3 irradiated with H^+ at energies of 500 keV, 640 keV and 2 MeV, the incident H^+ stops at the GaN film, GaN/Al_2O_3 heterojunction

and Al_2O_3 substrate, respectively. The yellow band and NBE are found in these three IBIL measurements, and they all drop with the fluence of H^+. Specifically, the NBE luminescence vanished at approximately 3×10^{12} ions/cm^2 when measured with 500 keV H^+ and at about 1×10^{13} ions/cm^2 when measured with 640 keV H^+. Interestingly, the central peak of the yellow band remained relatively consistent across the range of incident H^+ energies. While the luminescence of the yellow band disappeared during irradiation measured with 500 keV and 640 keV H^+, a weak intensity persisted when measured with 2 MeV H^+. Compared with the yellow band related to point defects, the NBE caused by excitons in IBIL is relatively weak due to the low concentration of excitons at room temperature. Since the IBIL spectrum reflects the *in situ* information about GaN during ion irradiation, a large number of defects are generated and gradually converge into large defect clusters to prevent luminescence with the fluence of H^+.

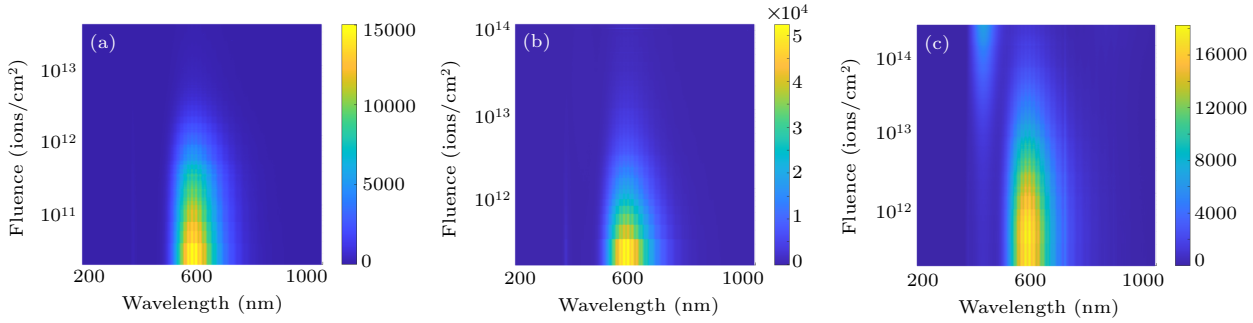


Fig. 3. *In situ* luminescence of GaN/Al_2O_3 measured with (a) 500 keV, (b) 640 keV and (c) 2 MeV H^+.

In comparison with the luminescence measurements using 500 keV and 640 keV H^+, a distinct and notable luminescence peak at 420 nm (2.95 eV) became evident when measured with 2 MeV H^+. Furthermore, the intensity of 420 nm (2.95 eV) luminescence exhibited an increase with the fluence of 2 MeV H^+. As the fluence of 2 MeV H^+ approached approximately 1×10^{13} ions/cm^2, the NBE band appeared to be encompassed within the broader 420 nm (2.95 eV) band. Additionally, there was also a small luminescence peak observed at 695 nm (1.78 eV), and this peak demonstrated a reduction in intensity with the fluence of 2 MeV H^+. These observations suggest that the defect responsible for the luminescence at 420 nm (2.95 eV) and 695 nm (1.78 eV) is primarily located within the Al_2O_3 substrate.

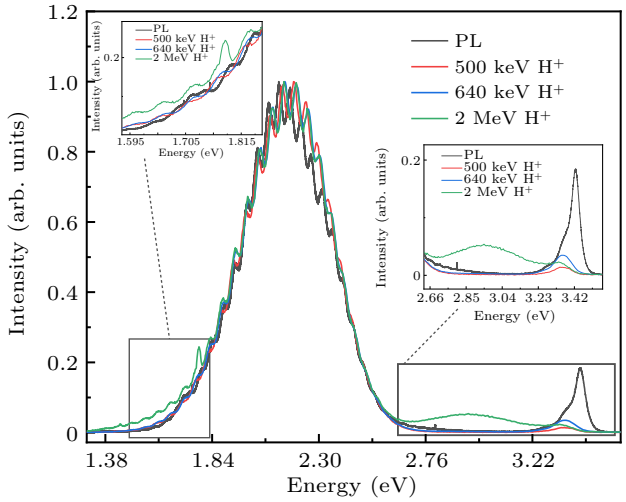


Fig. 4. Normalized comparison of the luminescence spectra measured with PL (obtained at 250 K) and IBIL (at room temperature).

PL experiments conducted at 250 K were performed as comparisons for the IBIL measurements, and the normalized spectrum was acquired for comparison, as shown in Fig. 4. It is important to note that the measurement depth in PL experiments within crystals is limited to the range of tens of nanometers to 1 μm from the surface, and does not reach the depth of the Al_2O_3 substrate. The center of the NBE is at 3.43 eV (PL at 250 K), 3.36 eV (IBIL with 500 keV H^+), 3.36 eV (IBIL with 640 keV H^+) and 3.34 eV (IBIL with 2 MeV H^+). Notably, the center of the NBE measured with 2 MeV H^+ is slightly lower than that measured with 500 keV H^+ and 640 keV H^+, a phenomenon attributed to the influence of 420 nm (2.95 eV) luminescence.

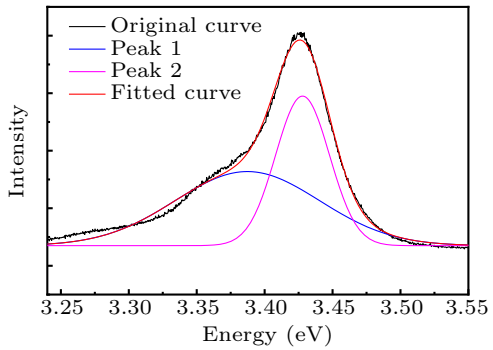


Fig. 5. A typical Gaussian decomposition of the PL spectrum of the GaN/Al_2O_3 sample (3.38 eV, 3.43 eV) measured at 250 K.

The NBE band observed in PL measurement is evidently asymmetric and can be decomposed into two peaks at 3.38 eV with a full width at half maximum (FWHM) of 0.0466 eV, and the other at 3.43 eV with a FWHM of 0.1254 eV, as shown in Fig. 5. These two Gaussian peaks are linked to the recombination of free excitons (FE) and excitons bound to neutral shallow donors (DX).[31] In these three IBIL measurements, FE

and DX merge into a wide band due to the nonradiative recombination of excitons at room temperature. The potential difference caused by surface charge accumulation can contribute to the separation of electron–hole pairs and influence the lifetime and migration of free excitons. It is important to recognize that the intensity of the IBIL measurement is predominantly associated with the energy of H^+ deposited in GaN.

The luminescence at the yellow band is attributed to the presence of several point defects and complexes. In previous studies, V_N, Si_{Ga} and O_N often acted as donor defects and V_{Ga}, Ga_i, N_{Ga} and the complex as acceptor defects. The recombination of donor and acceptor defects was suggested to be responsible for the yellow band,[4,27–30] but recent studies have shown that C_N defects may be responsible for the yellow luminescence.[8] It is worth noting that when comparing PL with IBIL measurements there is a slight deviation in the center of the yellow band luminescence towards higher energy with IBIL. This discrepancy can be attributed to the concentration distribution of defects. The yellow band is known to be inhomogeneous, and different measurement conditions, as well as the dynamic formation and interactions of defects during ion irradiation, can contribute to variations in the observed luminescence characteristics. There are several small peaks in yellow band due to the diffraction of interference layers.

The 420 nm luminescence peak only appears when measuring with 2 MeV H^+ and is unrelated to the GaN film. The dislocation defect of the GaN and Al_2O_3 heterojunction is not expected to appear in luminescence measurements.[8] The luminescence is consistent with F centers in Al_2O_3 typically arising from oxygen vacancies with two trapped electrons.[9–12] It is notable that this luminescence can be observed in both nonirradiated and various irradiated samples.[10,34] The radiation effect of the F center has been widely studied, and it increases with the fluence of ions at medium temperature due to the increase in oxygen vacancies during the irradiation.

In addition, luminescence at 695 nm was only found in the 2 MeV H^+ measurement, and is probably caused by the impurity Cr^{3+} ($^2E \rightarrow {}^4A_2$ radiative transition) in Al_2O_3. It is worth noting that this phenomenon is consistent with the work of Crespillo *et al.*, who also utilized 2 MeV H^+ to study the *in situ* luminescence of α-Al_2O_3 and observed a luminescence peak at 695 nm (1.78 eV),[34] This peak has been identified as being associated with the impurity Cr^{3+} in Al_2O_3.[35–37]

The normalized intensity for the center of the yellow band, as measured with 500 keV, 640 keV and 2 MeV H^+, is presented in Fig. 6. Although the luminescent components within the yellow band are relatively complex they are all related to point defects.[4,8,27–30] The intensity of the yellow band tends to exhibit a rapid initial decline, followed by a slower decline, and ultimately reaches a steady intensity level with the fluence of H^+. In the case of measurement with 2 MeV H^+, the yellow band luminescence persists throughout the entire irradiation process, disappearing at approximately 5×10^{12} ions/cm^2 and 5×10^{13} ions/cm^2 when measured with 500 keV and 640 keV H^+, respectively. During the initial stages of H^+ implantation, with the accumulation of injected ions, an increasing number of point defects are generated and begin to aggregate into large defect clusters. This process leads to a lattice structure damage, which in turn reduces the stress of ionic bonds and significantly diminishes the probability of capture of excitons by luminous centers. Consequently, this radiation effect results in a faster rate of luminescent decay and more rapid defect generation. The rate at which the yellow band intensity declines is notably faster in measurements with 500 keV H^+ compared with measurements with 640 keV and 2 MeV H^+. This discrepancy arises from the fact that the Bragg peak of 500 keV is at the GaN film and the Bragg peak of 640 keV and 2 MeV H^+ is within the Al_2O_3 substrate. According to results obtained by Agulló-López *et al.*, the average density of the electron–hole pairs generated by ionization is approximately 40% of the energy of incident ions.[32] The decline behaves as $R_{500\ \mathrm{keV}} > R_{640\ \mathrm{keV}} > R_{2\ \mathrm{MeV}}$ (R represents the rate of decline). Due to the direct radiation damage caused by nuclear stopping, the rate of decline of yellow band luminescence corresponds to the proportion of S_n for each energy.

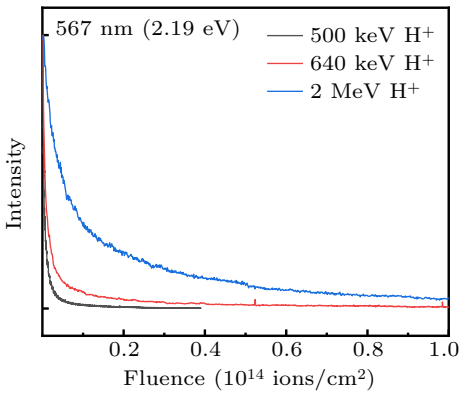


Fig. 6. The normalized spectrum of the yellow band luminescence measured with 500 keV, 640 keV and 2 MeV H^+.

The evolution of the NBE intensity, as measured with 500 keV, 640 keV and 2 MeV H^+, is shown in Fig. 7. The luminescence intensities measured with 500 keV and 640 keV H^+ show a decreasing trend with the fluence of H^+, and decrease rapidly at first and then slowly. From the previous SRIM simulation, it can be seen that a significant portion of H^+ energy is lost through ionization upon entering GaN/Al_2O_3. The NBE intensity is suppressed due to the substantial ionization of H^+, resulting in a rapid decrease in the number of excitons. Additionally, the presence of defect clusters may impede the mobility of excitons when measured by

IBIL.[34] For the 2 MeV H^+ measurement, the intensity of the NBE decreases at first and then grows stronger after the fluence of H^+ increases to 3×10^{12} ions/cm^2, which is due to the growth of the luminescence F centers at 420 nm.

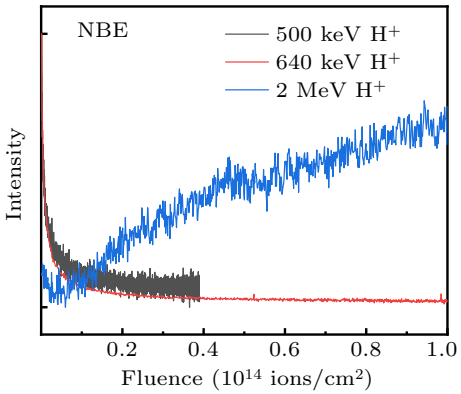


Fig. 7. The normalized spectrum of the NBE luminescence measured with 500 keV, 640 keV and 2 MeV H^+.

The spectra obtained with 2 MeV H^+ measurement at different fluences are shown in Fig. 8. The intensity of the yellow band decreases quickly. At the H^+ fluence reaches 2.05×10^{11} ions/cm^2, the intensity of yellow band is much larger than the F center and the NBE is clearly distinguishable. When the fluence reaches 3.08×10^{13} ions/cm^2, the intensity of the yellow band and F center become nearly equal and the NBE band can no longer be distinguished from the F center. In Fig. 9, it can be observed that the luminescence intensity at 3.34 eV, 1.78 eV and 2.19 eV (the center of the yellow band) decreases continuously with the fluence of H^+, while the luminescence at 420 nm (2.95 eV) increases gradually with the fluence of H^+. The FWHM of the F center increases and the position of the F center remains stable with the fluence of H^+. The intensity of the F center starts from a non-zero value, which indicates that there are already oxygen vacancies in Al_2O_3 before H^+ irradiation. During the early stage of irradiation, the intensity of the F center increases rapidly due to the oxygen vacancies, and interstitials are generated, caused by ionization and atomic displacements. The intensity of the F center reaches saturation at later stages of irradiation due to competition from non-radiative recombination mechanisms. The behavior of the F center with 2 MeV H^+ measurement indicates that the concentration of the F defect center increases with H^+ irradiation, which is consistent with findings from studies by Crespillo *et al.* and Kruzhalov *et al.*[10,34] The intensity of the F center surpasses that of the yellow band when the accumulated fluence is above 3.1×10^{13} ions/cm^2. In the study by Crespillo *et al.*,[34] the intensity of Cr^{3+} remains stable during irradiation, which is inconsistent with our result. The decrease of Cr^{3+} luminescence intensity in this measurement is due to the decrease of the yellow band in GaN film. Thus the trend of Cr^{3+} luminescence intensity behaves consistently with the behavior of the yellow band center with the fluence of H^+.

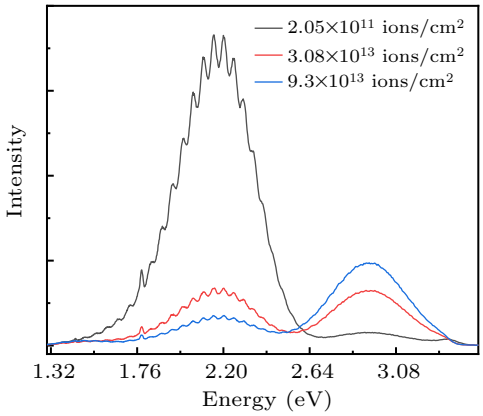


Fig. 8. Luminescence intensity at different fluences when measured with 2 MeV H^+.

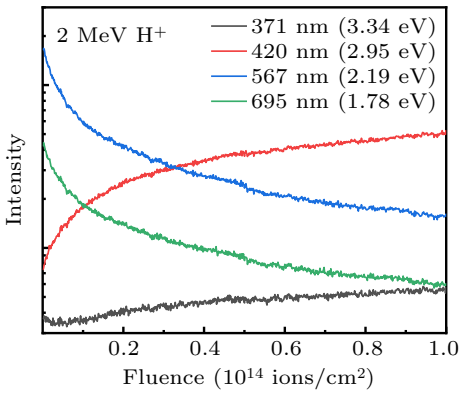


Fig. 9. Fluence evolution of the luminescence intensity at 3.34 eV, 2.95 eV, 1.78 eV and 2.19 eV when measured with 2 MeV H^+.

4. Conclusion

IBIL measurement provides a new method for studying materials with a complex structure, including GaN/Al_2O_3, and can provide information on every layer and construct a correlation of luminescence with defects in every layer. The IBIL spectra contain information on *in situ* luminescence and defects at a certain depth, neither of which cannot be acquired with PL measurements.

The IBIL spectra of GaN/Al_2O_3 were studied at 500 keV, 640 keV, and 2 MeV H^+. The luminescence at the yellow band caused by point defects decreases with the fluence of H^+ due to the congregation of point defects and the formation of nonradiative centers. The NBE band behaves as a wide band merged by FE and DX when measured with IBIL at room temperature. The rate of decline of yellow band intensity within GaN film corresponds to the proportion of nuclear stopping energy (S_n) with different incident ion energies. As a comparison for the IBIL measurement with 500 keV and 640 keV H^+, F centers at 2.95 eV and Cr^{3+} ($^2E\rightarrow{}^4A_2$ radiative transition) at 1.78 eV in Al_2O_3 were only measured with 2 MeV H^+. The luminescence intensity and FWHM of F centers all increase with the fluence of H^+. The intensity of Cr^{3+} luminescence shows a decline with the fluence of H^+, which corresponds to the yellow band center.

References

[1] DenBaars S P, Feezell D, Kelchner K, Pimputkar S, Pan C C, Yen C C, Tanaka S, Zhao Y J, Pfaff N, Farrell R, Iza M, Keller S, Mishra U, Speck J S and Nakamura S 2013 *Acta. Mater.* **61** 945

[2] Flack T J, Pushpakaran B N and Bayne S B 2016 *J. Electron. Mater.* **45** 2673

[3] Yanagida T, Kato T, Nakauchi D, Okada G and Kawaguchi N 2021 *Appl. Phys. Express.* **14** 082006

[4] Tung L T, Lin K L, Chang E Y, Huang W C, Hsiao Y L and Chiang C H 2009 *J. Phys.: Conf. Ser.* **187** 012021

[5] Reshchikov M A 2011 *Phys. Status. Solidi.* **8** 2136

[6] Reshchikov M A and Morkoç H 2005 *J. Appl. Phys.* **97** 061301

[7] Reshchikov M A, McNamara J D, Helava H, Usikov A and Makarov Y 2018 *Sci. Rep.* **8** 8091

[8] Reshchikov M A 2022 *Phys. Status. Solidi. (b)* **260** 2200488

[9] Popov A I, Lushchik A, Shablonin E, Vasil'chenko E, Kotomin E A, Moskina A M and Kuzovkov V N 2018 *Nucl. Instrum. Meth. B* **433** 93

[10] Kruzhalov A V, Milman I I, Ryabukhin O V, Revkov I G and Litovchenko E N 2010 *Radiat. Meas.* **45** 362

[11] Shablonin E, Popov A I, Prieditis G, Vasil'chenko E and Lushchik A 2021 *J. Nucl. Mater.* **543** 152600

[12] Makhov V N, Lushchik A, Lushchik C B, Kirm M, Vasil'chenko E, Vielhauer S, Harutunyan V V and Aleksanyan E 2008 *Nucl. Instrum. Meth. B* **266** 2949

[13] Malo M, Moroño A and Hodgson E R. 2014 *Fusion. Eng. Des.* **89** 2179

[14] Grygiel C, Moisy F, Sall M, Lebius H, Balanzat E, Madi T, Been T, Marie D and Monnet I 2017 *Acta Mater.* **140** 157

[15] Gonçalves K A, Bitencourt J F S, Mittani J C R and Tatumi S H 2010 *IOP Conf. Ser.: Mater. Sci. Eng.* **15** 012080

[16] Sarasola-Martin I, Correcher V and García-Guinea J 2021 *J. Alloys Compd.* **886** 161262

[17] Nakagawa T, Sakaguchi I, Shibata N, Matsunaga K, Mizoguchi T, Yamamoto T, Haneda H and Ikuhara Y 2007 *Acta Mater.* **55** 6627

[18] Branson J V, Hattar K, Rossi P, Vizkelethy G, Powell C J, Hernandez-Sanchez B and Doyle B L 2011 *Nucl. Instrum. Meth. B* **269** 2326

[19] Townsend P D 2012 *Nucl. Instrum. Meth. B* **286** 35

[20] Huddle J R, Grant P G, Ludington A R and Foster R L 2007 *Nucl. Instrum. Meth. B.* **261** 475

[21] Jiang W, Cheng W, Qiu M, Wu S, Ouyang X, Chen L, Pang P, Ying M and Liao B 2023 *Materials* **16** 2935

[22] Qiu M L, Yin P, Wang G F, Song J G, Luo C W, Wang T S, Zhao G Q, Lv S S, Zhang F S and Liao B 2020 *Chin. Phys. B* **29** 046106

[23] Wang T S, Wang G F, Qiu M L, Cheng W, Zhang J F and Zhao G Q 2021 *J. Lumin.* **237** 118133

[24] Luo C W, Qiu M L, Wang G F, Wang T S, Zhao G Q and Hua Q S 2020 *Acta Phys. Sin.* **69** 102901 (in Chinese)

[25] Song Y, Qiu M, Zhang J, Wu Y, Zhou M, Lin X and Wang G 2023 *Nucl. Instrum. Meth. B* **541** 392

[26] Qiu M L, Wang G F, Chu Y J, Zheng L, Xu M and Yin P 2017 *Acta Phys. Sin.* **66** 207801 (in Chinese)

[27] Soh C B, Chua S J, Lim H F, Chi D Z, Tripathy S and Liu W 2004 *J. Appl. Phys.* **96** 1341

[28] Reshchikov M A, McNamara J D, Helava H, Usikov A and Makarov Y 2018 *Sci. Rep.* **8** 8091

[29] Liu B, Yuan F, Dierre B, Sekiguchi T, Zhang S, Xu Y and Jiang X 2014 *ACS Appl. Mater. Interface* **6** 14159

[30] Reshchikov M A, Demchenko D O, Usikov A, Helava H and Makarov Y 2014 *Phys. Rev. B* **90** 235203

[31] Monemar B, Paskov P P, Bergman J P, Toropov A A, Shubina T V, Malinauskas T and Usui A 2008 *Phys. Status. Solidi. (b)* **245** 1723

[32] Agulló-López F, Climent-Font A, Muñoz-Martín Á, Olivares J and Zucchiatti A 2016 *Prog. Mater. Sci.* **76** 1

[33] Reshchikov M A and Korotkov R Y 2001 *Phys. Rev. B* **64** 115205

[34] Crespillo M L, Graham J T, Zhang Y and Weber W J 2016 *J. Lumin* **172** 208

[35] Adachi S 2021 *Opt. Mater.* **114** 111000

[36] Lee K H and Crawford J H 1979 *Phys. Rev. B* **19** 3217

[37] Lewis P M, Keerthana N, Deepak H N, Choudhari K S and Kulkarni S D 2021 *Curr. Appl. Phys.* **32** 71